



Comparison of FTIR spectrum with chemometric and machine learning classifying analysis for differentiating guan-mutong a nephrotoxic and carcinogenic traditional chinese medicine with chuan-mutong

Chu Shan Tan ^a, Shin Yee Leow ^a, Chen Ying ^b, Choo Jun Tan ^c, Tiem Leong Yoon ^d,
Chen Jingying ^{e,*}, Mun Fei Yam ^{a,f,*}

^a School of Pharmaceutical Sciences, Universiti Sains Malaysia, 11800 Penang, Malaysia

^b School of Traditional Chinese Medicine, Beijing University of Chinese Medicine, Beijing 102488, China

^c School of Science and Technology, Wawasan Open University, 54, Jalan Sultan Ahmad Shah, 10050 Penang, Malaysia

^d School of Physics, Universiti Sains Malaysia, 11800 Penang, Malaysia

^e Research Center for Medicinal Plant, Institute of Agricultural Bio-resource, Fujian Academy of Agricultural Sciences, Fuzhou 350003, Fujian, China

^f College of Pharmacy, Fujian University of Traditional Chinese Medicine, 1 Qiyang Road, Shangjie, Minhou, Fuzhou 350122, Fujian, China



ARTICLE INFO

Keywords:

Mutong
Tri-step Fourier Transform Instruments (FT-IR)
PLS-DA
Machine learning
PCA analysis
Herbal adulteration

ABSTRACT

Chuan-Mutong (*Clematis* spp.) is a precious medicinal herb in traditional Chinese medicine that possesses various therapeutic effects especially well known for its diuretic effect and widely used in Malaysia. However, there were several reported Chinese herb nephropathy cases due to the adulteration of *Aristolochia* spp. found in combinational herbal regimen. Guan-Mutong (*Aristolochia manshuriensis*), which looks similar in appearance and has similar therapeutic effects as Chuan-Mutong, has the possibility to substitute the Chuan-Mutong. Therefore, there is a necessity to differentiate the types of Mutong using analytical authentication methods. In this paper, a rapid and accurate method is proposed to discriminate Chuan-Mutong from Guan-Mutong by using tri-step fourier transform infrared spectroscopy (FT-IR) identification approaches. The method involves the deployment of FT-IR, second derivative infrared spectra (SD-IR), and two-dimensional correlation infrared spectra (2D-IR). In our approach, FT-IR spectra of Chuan-Mutong and Guan-Mutong were subjected to discrimination using principal component analysis (PCA), partial least squares discriminant analysis (PLS-DA), and machine learning classifiers (ML). Chuan-Mutong and Guan-Mutong can be clearly classified or discriminated against each other by ML, PLS-DA and PCA. The sensitivity, accuracy and specificity of ML were >90%, while the sensitivity, accuracy and specificity of PLS-DA were 100%. It is hence demonstrated that the infrared spectroscopic identification approach using PCA, PLS-DA and ML can be effectively used to differentiate Chuan-Mutong and Guan-Mutong. PLS-DA and ML provide a simple, fast, and high accuracy prediction to differentiate Chuan-Mutong and Guan-Mutong.

1. Introduction

Mutong or *Akebia species* is a precious traditional Chinese medicinal herb that possesses various therapeutic effects especially well known for its diuretic effect as mention in Chinese Pharmacopeia [1,2]. It is widely distributed in East Asia especially in China, Japan, and Korea. Its dried stems have been often used as the remedy in traditional medical treatment due to its antiphlogistic, diuretic, and analgesic properties [3]. Moreover, it has anti-inflammatory properties which provides favorable

effects in urinary tract inflammation and eczema treatment [4]. The fruit has been applied in oriental medicine to cure urinary tract inflammatory disease, edema, prostatitis, obesity, urinary incontinence, and dysuria. It is also used for promoting blood circulation in traditional Chinese medicine [3]. Currently, several types of Mutong have been distributed in the market such as Mutong (*Akebiae caulis*), Guan-Mutong (*Aristolochia manshuriensis*), and Chuan-Mutong (*Clematis caulis*).

The classification of Mutong, Chuan-Mutong, and Guan-Mutong has varied throughout the history due to their similar physical appearance

* Corresponding authors at: School of Pharmaceutical Sciences, Universiti Sains Malaysia, 11800 Penang, Malaysia (M.F. Yam) and Research Center for Medicinal Plant, Institute of Agricultural Bio-resource, Fujian Academy of Agricultural Sciences, Fuzhou 350003, Fujian China (C. Jingying).

E-mail addresses: chenjy@faas.cn (C. Jingying), yammunfei@usm.my (M.F. Yam).

and pharmacological actions. The origin of Mutong can be traced to the Han Dynasty, and was known as 'Tong Cao' in *Shen Nong Ben Cao Jing*. However, in the Song Dynasty, Mutong and Tong Cao were mixed up until the Yuan Dynasty. The Mutong species were confirmed in the Ming Dynasty. There were many sub-species of Mutong that were derived during the Qing Dynasty [5]. Because of this complicated process and change of Dynasty, it leads to confusion of the real Mutong species.

In the year 1995, Guan-Mutong and Chuan-Mutong were both reported in Chinese Pharmacopeia. The first existence of Guan-Mutong was recorded in Dong Bei Yao Yong Zhi Wu Zhi (Zhu, 2002). An incident of renal intoxication with Chinese herb *Aristolochia* sp. (later known as the aristolochic acid nephropathy (AAN) incident) occurred in Belgium, France, Japan, Germany, UK and China around year 2000 [5]. After the incident, many countries such as Australia, United Kingdom, Canada, Europe, and the United States started to prohibit the usage of *Aristolochia* species in any medicinal and cosmetics [6–9]. The AAN incident caused concern over the safety of Guan-Mutong which also belongs to the *Aristolochia* family. Guan-Mutong was reported as a nephrotoxic and carcinogenic agent due to the presence of aristolochic acid [5]. Even though Guan-Mutong was excluded from Chinese Pharmacopeia, but TCM practitioners from some countries still prescribed it. Guan-Mutong is also available in local medical halls in these countries. In Malaysia, due to the scarcity of experts in TCM material medica, the society can hardly combat the adulteration of the unwanted herb in the market. This is especially so for Guan-Mutong which looks highly like Mutong. Besides, the pharmacological action and its clinical uses of Guan-Mutong in TCM are like Mutong and Chuan-Mutong. Substitution and adulteration of Guan-Mutong with Mutong or Chuan-Mutong present a potential health risk to the consumers. The confusion in discriminating these three types of Mutong is not merely due to their names in Chinese medicine but also to their common name [10,11]. In Malaysia, since there is no official authority responsible for validating the authenticity of the types of Mutong sold in TCM medical halls, reported cases of Guan-Mutong substituting Chuan-Mutong will continue to happen among the society. Based on the samples collected from medical halls throughout Malaysia during this study, no sample of Mutong (*Akrebia* spp.) was identified, inferring that such species are not commonly found in the medical halls in Malaysia.

Our study aims to categorize the Chuan-Mutong and Guan-Mutong samples using FT-IR with principal component analysis (PCA), and partial least squares discriminant analysis (PLS-DA) analysis methods. In addition, machine learning (ML) classifies analysis (RBF classifier, random forest, and J48) was also used to classify the spectra of Chuan-Mutong and Guan-Mutong. The outcome from ML was compared to that from the PLS-DA analysis.

2. Methodology

2.1. Apparatus

A Fourier Transform Infrared (FT-IR) Spectrometer (Perkin Elmer, USA), equipped with a Deuterated Tri-Glycine Sulfate (DTGS) detector was used to determine the spectra of each sample taken at different temperatures. A programmable temperature controller (Model GS20730, Specac, UK) was used to perform the thermal perturbation with 10 °C intervals (from 20 °C–120 °C) to obtain the reading. A stainless-steel mesh (200-mesh size) was used to sieve and grind sample powder.

2.2. Materials

A total of 164 samples of Mutong (either Guan-Mutong or Chuan-Mutong) was collected from 13 states in Malaysia and China. After carefully inspected by experts, it was concluded that the samples comprise of 56 Guan-Mutong and 108 Chuan-Mutong. Moreover, Mutong and Chuan-Mutong standard reference herb was purchased

Table 1
The information of samples collected from Malaysia and China.

No.	Label	Location/ Province	State/ Country	Type
1	NS01	Seremban	Negeri Sembilan	Chuan-Mutong
2	NS02	Seremban	Negeri Sembilan	Guan-Mutong
3	NS03	Seremban	Negeri Sembilan	Chuan-Mutong
4	NS04	Seremban	Negeri Sembilan	Chuan-Mutong
5	NS05	Seremban	Negeri Sembilan	Chuan-Mutong
6	NS06	Port Dickson	Negeri Sembilan	Guan-Mutong
7	NS07	Port Dickson	Negeri Sembilan	Chuan-Mutong
8	NS08	Seremban	Negeri Sembilan	Chuan-Mutong
9	NS09	Lukut	Negeri Sembilan	Guan-Mutong
10	NS10	Port Dickson	Negeri Sembilan	Chuan-Mutong
11	NS11	Port Dickson	Negeri Sembilan	Chuan-Mutong
12	NS12	Bukit Pelendok	Negeri Sembilan	Guan-Mutong
13	NS13	Bahau	Negeri Sembilan	Chuan-Mutong
14	NS14	Bahau	Negeri Sembilan	Chuan-Mutong
15	NS15	Bukit Pelendok	Negeri Sembilan	Chuan-Mutong
16	NS16	Seremban	Negeri Sembilan	Chuan-Mutong
17	NS17	Seremban	Negeri Sembilan	Chuan-Mutong
18	NS18	Seremban	Negeri Sembilan	Chuan-Mutong
19	PH01	Kuantan	Pahang	Chuan-Mutong
20	PH02	Kuantan	Pahang	Chuan-Mutong
21	PH03	Kuantan	Pahang	Chuan-Mutong
22	PH04	Kuantan	Pahang	Guan-Mutong
23	PH05	Kuantan	Pahang	Chuan-Mutong
24	PH07	Kuantan	Pahang	Guan-Mutong
25	PH08	Kuantan	Pahang	Chuan-Mutong
26	PH09	Kuantan	Pahang	Chuan-Mutong
27	PH10	Kuantan	Pahang	Chuan-Mutong
28	PH11	Kuantan	Pahang	Chuan-Mutong
29	PH12	Kuantan	Pahang	Guan-Mutong
30	PH13	Kuantan	Pahang	Guan-Mutong
31	PH14	Kuantan	Pahang	Chuan-Mutong
32	PH15	Kuantan	Pahang	Chuan-Mutong
33	PH16	Kuantan	Pahang	Chuan-Mutong
34	PH17	Kuantan	Pahang	Chuan-Mutong
35	PH18	Kuantan	Pahang	Chuan-Mutong
36	PK01	Ipooh	Perak	Guan-Mutong
37	PK02	Ipooh	Perak	Chuan-Mutong

(continued on next page)

Table 1 (continued)

No.	Label	Location/ Province	State/ Country	Type
38	PK03	Sungai Siput	Perak	Chuan-Mutong
39	PK04	Ipoh	Perak	Chuan-Mutong
40	PK05	Kampar	Perak	Guan-Mutong
41	PK06	Kampar	Perak	Chuan-Mutong
42	PK07	Taiping	Perak	Guan-Mutong
43	PK08	Taiping	Perak	Chuan-Mutong
44	PK09	Sungai Siput	Perak	Guan-Mutong
45	PK10	Bagan Serai	Perak	Chuan-Mutong
46	PK11	Ipoh	Perak	Chuan-Mutong
47	PK12	Ipoh	Perak	Chuan-Mutong
48	PK13	Sitiawan	Perak	Chuan-Mutong
49	PK14	Sitiawan	Perak	Guan-Mutong
50	PK15	Sitiawan	Perak	Chuan-Mutong
51	PK16	Ayer Tawar	Perak	Guan-Mutong
52	PK17	Sitiawan	Perak	Chuan-Mutong
53	PK18	Sitiawan	Perak	Chuan-Mutong
54	PK19	Sitiawan	Perak	Chuan-Mutong
55	PK20	Sitiawan	Perak	Guan-Mutong
56	P01	Kangar	Perlis	Guan-Mutong
57	PP01	Bukit Mertajam	Penang	Guan-Mutong
58	PP02	Georgetown	Penang	Guan-Mutong
59	PP03	Georgetown	Penang	Chuan-Mutong
60	PP04	Georgetown	Penang	Guan-Mutong
61	PP05	Georgetown	Penang	Chuan-Mutong
62	PP06	Georgetown	Penang	Chuan-Mutong
63	PP07	Georgetown	Penang	Guan-Mutong
64	PP08	Georgetown	Penang	Chuan-Mutong
65	PP09	Georgetown	Penang	Guan-Mutong
66	PP10	Kepala Batas	Penang	Chuan-Mutong
67	PP12	Kepala Batas	Penang	Guan-Mutong
68	PP14	Air Itam	Penang	Guan-Mutong
69	PP15	Georgetown	Penang	Chuan-Mutong
70	PP16	Georgetown	Penang	Guan-Mutong
71	M01	Bukit Beruang	Melaka	Guan-Mutong
72	M02	Bukit Beruang	Melaka	Guan-Mutong
73	SK01	Sarikei	Sarawak	Guan-Mutong
74	SB02	Kota Kinabalu	Sabah	

Table 1 (continued)

No.	Label	Location/ Province	State/ Country	Type
75	SB03	Kota Kinabalu	Sabah	Chuan-Mutong
76	T01	Kemaman	Terengganu	Chuan-Mutong
77	J01	Kota Tinggi	Johor	Guan-Mutong
78	J02	Muar	Johor	Guan-Mutong
79	J03	Skudai	Johor	Guan-Mutong
80	J04	Skudai	Johor	Chuan-Mutong
81	J05	Muar	Johor	Chuan-Mutong
82	J06	Johor Bharu	Johor	Chuan-Mutong
83	J07	Johor Bharu	Johor	Guan-Mutong
84	J08	Skudai	Johor	Guan-Mutong
85	J09	Johor Bharu	Johor	Chuan-Mutong
86	J10	Johor Bharu	Johor	Chuan-Mutong
87	J11	Johor Bharu	Johor	Guan-Mutong
88	J12	Johor Bharu	Johor	Chuan-Mutong
89	J13	Johor Bharu	Johor	Chuan-Mutong
90	KT01	Kota Bharu	Kelantan	Chuan-Mutong
91	KT02	Kota Bharu	Kelantan	Chuan-Mutong
92	KT03	Kota Bharu	Kelantan	Guan-Mutong
93	KT04	Kota Bharu	Kelantan	Chuan-Mutong
94	KL01	Kepong	Kuala Lumpur	Chuan-Mutong
95	KL02	Sungai Long	Kuala Lumpur	Guan-Mutong
96	KL03	Sungai Long	Kuala Lumpur	Chuan-Mutong
97	KL04	Cheras	Kuala Lumpur	Guan-Mutong
98	KL05	Cheras	Kuala Lumpur	Chuan-Mutong
99	KL06	Kuala Lumpur	Kuala Lumpur	Guan-Mutong
100	KL07	Kuala Lumpur	Kuala Lumpur	Chuan-Mutong
101	KL08	Cheras	Kuala Lumpur	Guan-Mutong
102	KL09	Cheras	Kuala Lumpur	Chuan-Mutong
103	KL10	Cheras	Kuala Lumpur	Guan-Mutong
104	S01	Cheras	Selangor	Chuan-Mutong
105	S02	Cheras	Selangor	Guan-Mutong
106	S03	Cheras	Selangor	Chuan-Mutong
107	S04	Kajang	Selangor	Guan-Mutong
108	S05	Kajang	Selangor	Chuan-Mutong
109	S06	Cheras	Selangor	Chuan-Mutong
110	S07	Cheras	Selangor	Guan-Mutong
111	S08	Sungai Pelek	Selangor	Chuan-Mutong

(continued on next page)

Table 1 (continued)

No.	Label	Location/ Province	State/ Country	Type
112	S09	Sungai Pelek	Selangor	Chuan-Mutong
113	S10	Banting	Selangor	Chuan-Mutong
114	S11	Banting	Selangor	Chuan-Mutong
115	S12	Tanjong Sepat	Selangor	Chuan-Mutong
116	S13	Sungai Pelek	Selangor	Chuan-Mutong
117	S14	Sepang	Selangor	Chuan-Mutong
118	S15	Serendah	Selangor	Guan-Mutong
119	S16	Tanjung Sepat	Selangor	Guan-Mutong
120	S17	Sepang	Selangor	Chuan-Mutong
121	S18	Ampang	Selangor	Guan-Mutong
122	S19	Kajang	Selangor	Chuan-Mutong
123	S20	Ampang	Selangor	Guan-Mutong
124	K01	Sungai Petani	Kedah	Guan-Mutong
125	K02	Alor Setar	Kedah	Guan-Mutong
126	K03	Alor Setar	Kedah	Chuan-Mutong
127	K04	Alor Setar	Kedah	Guan-Mutong
128	K05	Alor Setar	Kedah	Guan-Mutong
129	K06	Alor Setar	Kedah	Chuan-Mutong
130	K07	Alor Setar	Kedah	Guan-Mutong
131	K08	Alor Setar	Kedah	Guan-Mutong
132	K09	Alor Setar	Kedah	Chuan-Mutong
133	K10	Alor Setar	Kedah	Guan-Mutong
134	K11	Alor Setar	Kedah	Chuan-Mutong
135	K12	Alor Setar	Kedah	Guan-Mutong
136	K13	Alor Setar	Kedah	Chuan-Mutong
137	K14	Alor Setar	Kedah	Chuan-Mutong
138	K15	Alor Setar	Kedah	Guan-Mutong
139	K16	Alor Setar	Kedah	Guan-Mutong
140	C01	Guang Dong	China	Chuan-Mutong
141	C02	Guang Dong	China	Chuan-Mutong
142	C03	Dao Di Tang	China	Chuan-Mutong
143	C04	Guang Dong	China	Chuan-Mutong
144	C05	Zhe Jiang	China	Chuan-Mutong
145	C06	Ning Shi	China	Chuan-Mutong
146	C07	Jian Shui Tang	China	Chuan-Mutong
147	C08	Guang Dong	China	Chuan-Mutong
148	C09	Si Chuan	China	Chuan-Mutong

Table 1 (continued)

No.	Label	Location/ Province	State/ Country	Type
149	C10	Sun Wan Dong	China	Chuan-Mutong
150	C11	An Wei	China	Chuan-Mutong
151	C12	Guang Dong	China	Chuan-Mutong
152	C13	Guai Li Gu Duo	China	Chuan-Mutong
153	C14	Hao Zhou	China	Chuan-Mutong
154	C15	Gui Zhou	China	Chuan-Mutong
155	C17	Guang Dong	China	Chuan-Mutong
156	C18	An Wei	China	Chuan-Mutong
157	C19	Hao Zhou	China	Chuan-Mutong
158	C20	An Guo Shi	China	Chuan-Mutong
159	C21	Dong Wan	China	Chuan-Mutong
160	C22	An Wei	China	Chuan-Mutong
161	C23	An Wei	China	Chuan-Mutong
162	STD01	Fujian Academy of Agricultural Sciences (Fuzhou, China)	China	Chuan-Mutong
163	C16	Fujian Academy of Agricultural Sciences (Fuzhou, China)	China	Guan-Mutong
164	121409–201402	National Institute for Food and Drug Control (Beijing, China)	China	Chuan-Mutong
165	STD02*	Fujian Academy of Agricultural Sciences (Fuzhou, China)	China	Mutong (Akrebia sp)

* indicates the sample only subjected for macroscopic analysis.

from the National Institute for Food and Drug Control (Beijing, China) with a serial number (121409–201402), Mutong (Akrebia caulis) and Guan-Mutong reference herb was supplied by Prof Chen Jingying (from Institute of Agricultural Bio-resource, Fujian Academy of Agricultural Sciences, China). Potassium Bromide (KBr) which is used in the FT-IR analysis was purchased from Merck (Germany). All the samples were listed in Table 1.

2.3. Macrostructure study of different types of Mutong

To assure their authenticity, the macrostructures of all raw herb samples were examined before grinding. Macroscopic authentication was manually carried out via careful visual inspection. The raw herbs were identified according to the TCM identification guides [1,12,13]. The morphology of each herb was carefully observed and compared to the reference atlas. Each herbal was then ground into powder form by using an herbal grinder (Yongli YF3-1, Zhejiang, China).

2.4. Conventional FTIR analysis

The KBr powder was initially dried in the oven at 120 °C one day prior to the FT-IR analysis to remove the water that may be present in it. Each dried sample was ground into fine powders using a blender separately and screened using a 200-mesh stainless steel sieve before putting them into the oven at temperature 45 °C for 48 h to remove the water contained in the samples. The samples were then mixed with KBr and pressed under high pressure (<10 mPa) into a pellet. Plain KBr pellet

Table 2
Machine learning classifiers.

Classifier	Type of classifier	Reference
J48	Decision Tree	[16]
RandomForests	Ensemble-based Decision Tree	[17]
RBFClassifier	Artificial Neural network	[18]

was used as the background of the spectrum. The sample pellet was placed into the sample holder in the spectrometer and analyzed. The temperature controller was adjusted from 20 °C to 120 °C at an interval of 10 °C to obtain a series of dynamic spectra for each sample. A total of 16 FT-IR spectrum was recorded for each sample to ameliorate the signal-to-noise ratio (SNR) and enhance the spectrum quality. The spectrum was scanned in the range of 400–4000 cm⁻¹ with resolution 4 cm⁻¹cm⁻¹ and 1 cm⁻¹ intervals. The effect of water and carbon dioxide was eliminated during the scanning process. The spectrum of the CO²- and H₂O-free absorbance curve for the sample was then obtained [14,15].

2.5. SD-IR, 2D-ID and PCA analysis

After obtaining the raw FT-IR data of the samples (CO²- and H₂O-free absorbance curve), they were processed using the Spectrum software, version 10.5.3 (Perkin Elmer Inc, USA). SD-IR spectra were obtained after baseline correction, normalization, and Savitzky-Golay polynomial fitting (13-point smoothing) at 20 °C. The synchronous two-dimensional IR (2D-IR) correlation analysis software developed by Tsinghua University, Beijing, China was used to calculate the spectra of 2D-IR correlation [14,15].

2.6. Chemometric analysis

Unsupervised pattern recognition techniques, named principal

component analysis (PCA) was applied as preliminary step to explore differences between the spectral of Guan-Mutong and Chuan-Mutong. After PCA analysis, partial least squares-discriminant analysis (PLS-DA) a supervised pattern recognition analysis was adapted for discrimination study. When conducting PLS-DA model, 60% of the spectra from Guan-Mutong and Chuan-Mutong were considered as a calibration set, and the remaining spectra were considered as a validation set. R²Y (percent of variation of the calibration set-Y, explained by the model), Q²Y (present of variation of calibration set-Y, predicted by the model according to cross validation), root mean square error of estimation (RMSEE), root mean squared error of cross validation (RMSECV), and root mean square error of cross validation (RMSEV) were calculated. Permutation test was performed as internal validation, the number of permutation was set as 100. In addition, three parameters, sensitivity, specificity and accuracy were determined to evaluate the performance of calibration model. All PLS-DA and PCA models were established by SIMCA 14.1 (Umetrics, Sweden) [16].

2.7. Machine learning classification of the samples

This section presents the experimental studies with machine learning classifiers. A classifier assigns a class (categorical) label to an input. In the experiment, the adopted classifier was able to predict the labels of the data samples as either Guan-Mutong or Chuan-Mutong. There are three classifiers adopted as in Table 2.

A total of 164 data samples (measured at 20 °C) were used for evaluation using the *k*-fold cross-validation method. The method partitions all data samples into *k* (approximately) equal sub-sets. During the evaluation, (*k* - 1) sub-sets were used as the training set, and the remaining one was used as the test set. This evaluation procedure was repeated *k* times, whereby each sub-set was used as the test set once. In the experimental study, the (*k* = 10)-fold cross-validation method was repeated 30 times to estimate the accuracy of the classification

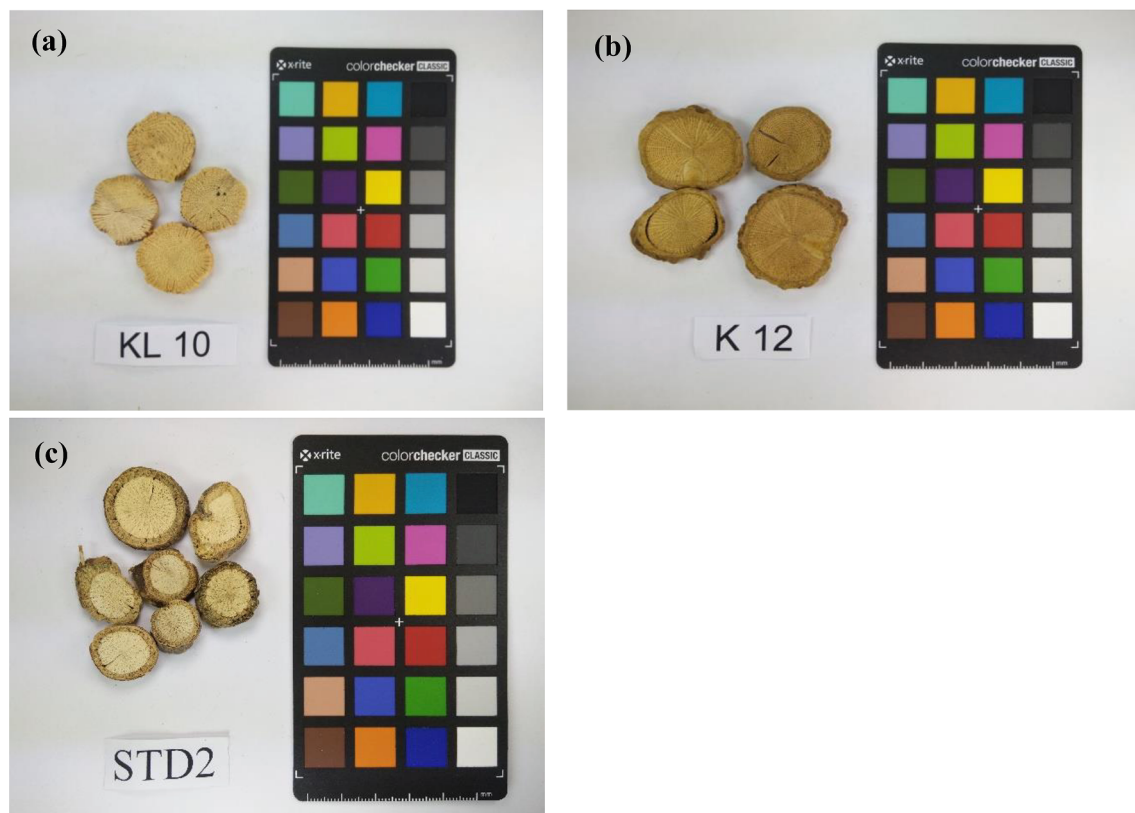


Fig. 1. Images of counterfeit species of Mutong from Malaysia and China: (a) KL10, (b) K12, and (c) STD2.

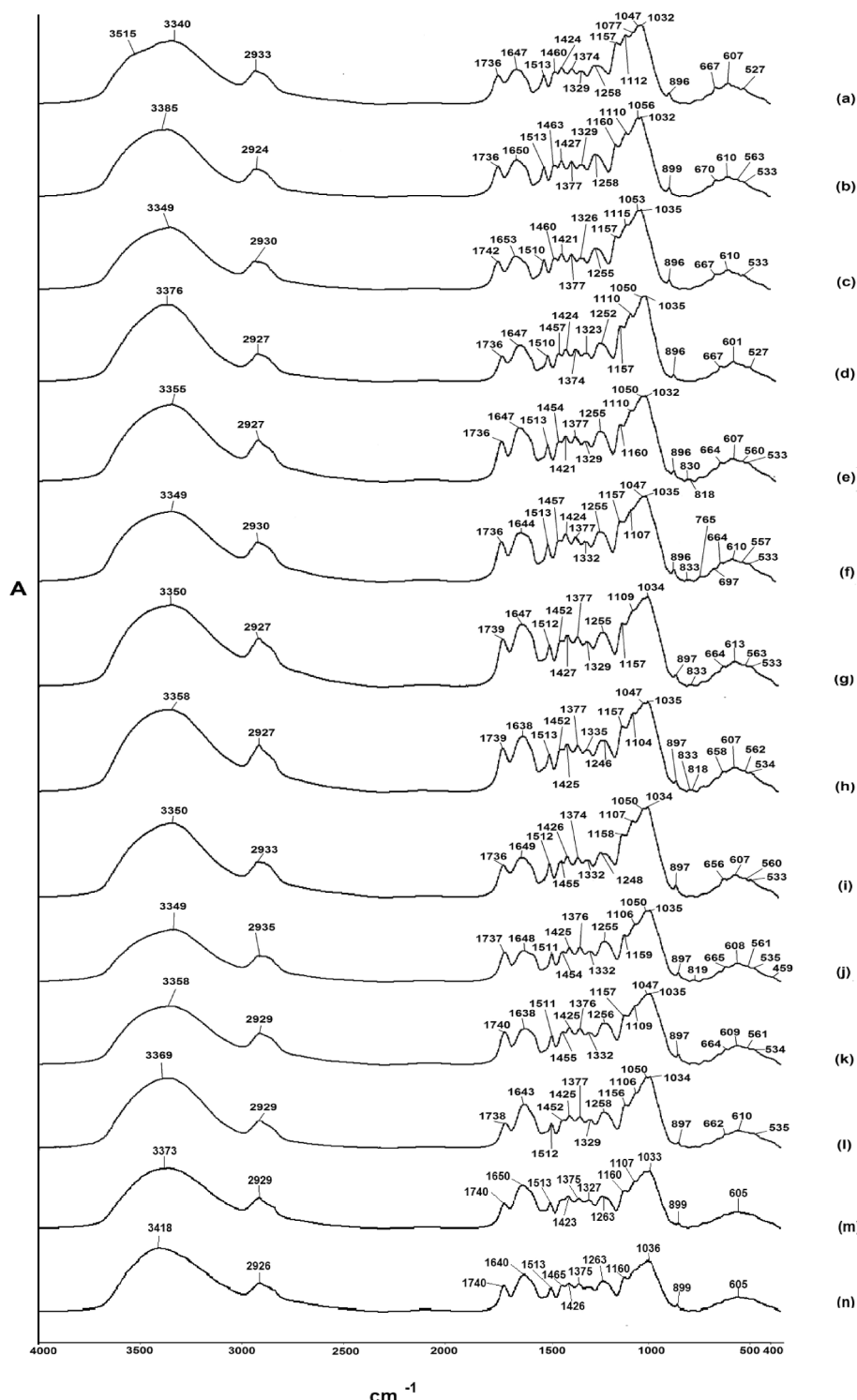


Fig. 2. FT-IR spectrum of Chuan-Mutong from Malaysia and China: (a) T01, (b) S08, (c) SB02, (d) PP05, (e) PK13, (f) PH08, (g) NS10, (h) KL10, (i) KT04, (j) K09, (k) J10, (l) C13, (m) STD 01, (n) NFDC (National Institute for Food and Drug Control (Beijing, China)).

performance on the Guan-Mutong and Chuan-Mutong data set [17–19].

3. Result and discussion

3.1. Macrostructure study

After carefully evaluating the macrostructure of the collected samples, none of the samples belong to *Akrebia* sp. Mutong. Among the

samples, 107 (107 sampling samples, 1 standard herb in powder purchased from National Institute for Food and Drug Control) and 56 samples were classified as Chuan-Mutong and Guan-Mutong, respectively.

Chuan-Mutong mostly had a cross-section of 2–3.5 cm in diameter. The bark had yellowish-brown, wood pale yellowish-brown and pale yellow, scattered black-brown spots. The texture was hard and not easily broken. The edges had uneven fracture, visible radial patterns, with

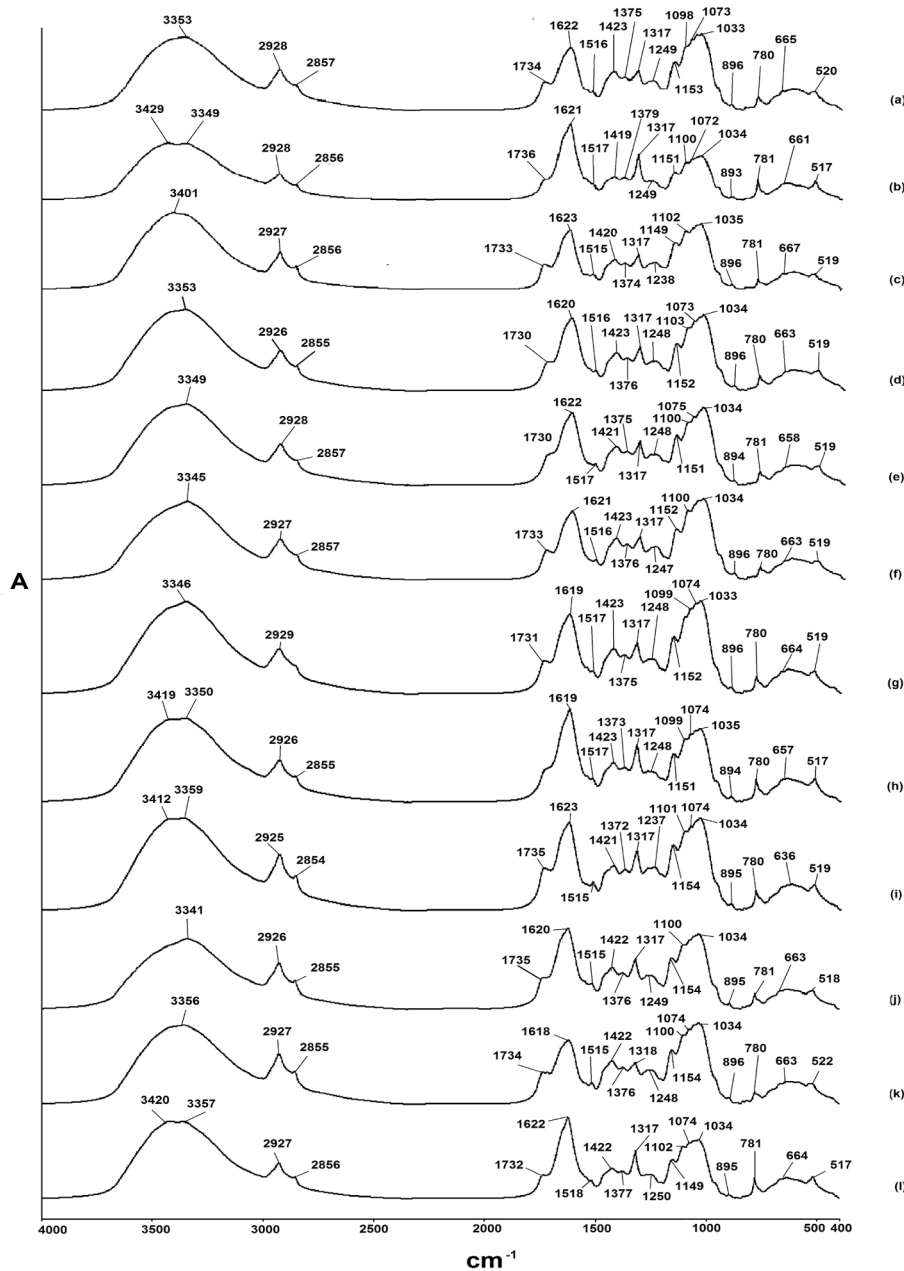


Fig. 3. FT-IR spectrum of Guan-Mutong from Malaysia and China: (a) S07, (b) PP07, (c) P01, (d) PK14, (e) NS13, (f) M01, (g) KT03, (h) PH07, (i) KL06, (j) K12, (k) J11, (l) C16.

vessel pores varying in size and scattered densely; the pith was whitish or yellowish-brown in color. The odor was slight, and the taste was slightly bitter (Fig. 1(a)).

The samples of Guan-Mutong had a cross-section of 2–4 cm in diameter. It was light but the texture was hard, pale yellow or yellow in color, narrow in the bark, and predominantly woody. They had multiple layers of neatly arranged vessels with white medulla ray in most of the vessels in the form of pinholes, or multiple concentric rings arranged in arachnid form. The odor was slight, and the taste was bitter (Fig. 1(b)).

The appearance of Mutong (*Akrebia* spp) was apparently different. Its texture was compact and fracture uneven. Its bark was yellowish-brown, woody or yellowish-white in color, rays are arranged radially with small pith. It had odor and a slight taste, slightly bitter and astringent (Fig. 1(c)).

3.2. Discrimination of Chuan-Mutong and Guan-Mutong by FT-IR analysis

Tri-step FT-IR identification consists of conventional infrared spectroscopy, second derivative infrared spectroscopy (SD-IR), and two-dimensional correlation infrared (2D-IR) spectroscopy which aims to interpret accumulative peaks from the spectra of each individual chemical components to provide a holistic chemical fingerprint of Chuan-Mutong and Guan-Mutong. Conventional infrared spectroscopy is a qualitative method to identify absorption peaks based on respective chemical components from the spectrum obtained. FT-IR spectrometers have more advantages as compared to traditional dispersive infrared instrumentation. FT-IR has a multiplex advantage where it allows multiple scans of the spectrum to be completed within a short period of time. It does not separate energy into individual frequencies for measurement. Hence it is a fast process. FT-IR allows more light, hence more energy to

pass through the sample and hit the detector in the FT-IR spectrometer as compared to traditional dispersive infrared instrumentation. This results in a higher signal-to-noise ratio which provides more sensitive and accurate absorption peaks found in the spectrum of each sample component.

Chuan-Mutong and Guan-Mutong samples were compared with the standard sample of Guan-Mutong (C-16) (sourced from Fujian Academy of Agricultural Sciences) and Chuan-Mutong (sourced from Fujian Academy of Agricultural Sciences and National Institute (STD01) and National Institute for Food and Drug Control (121409–201402)) were used as a reference to confirm the authenticity of samples. The conventional FT-IR spectrum of the Chuan-Mutong and Guan-Mutong samples were shown in Figs. 2 and 3, respectively.

Based on the FT-IR spectrum of 14 Chuan-Mutong samples, there were several similar main absorption bands as compared to the standard herbs. They show a strong and broad peak around $3385 \sim 3340 \text{ cm}^{-1}$ due to stretching vibration of O-H groups, $2933 \sim 2927 \text{ cm}^{-1}$ correspond to methylene ($-\text{CH}_2$) asymmetric stretching vibration, $1742 \sim 1736 \text{ cm}^{-1}$ were attributed to amide ($\text{C}=\text{O}$) stretching vibrations, $1653 \sim 1638 \text{ cm}^{-1}$ assigned to O-H bending, $1513 \sim 1510 \text{ cm}^{-1}$ were due to aromatic skeletal stretching vibration, ~ 1455 , ~ 1375 and $\sim 1330 \text{ cm}^{-1}$ contributed to C-H bending, $1258 \sim 1246 \text{ cm}^{-1}$ from the C-O-C stretching vibration, ~ 1156 , ~ 1109 , $\sim 1038 \text{ cm}^{-1}$ might be due to C-O stretching vibration (Table 2) [20,21].

Fig. 3 shows the FT-IR of Guan-Mutong samples. There were several similar main absorption bands such as strong and broad peak around $3359 \sim 3341 \text{ cm}^{-1}$ due to stretching vibration of O-H groups, $\sim 2927 \text{ cm}^{-1}$ correspond to methylene ($-\text{CH}_2$) asymmetric stretching vibration, $\sim 1736 \text{ cm}^{-1}$ were attributed to amide ($\text{C}=\text{O}$) stretching vibrations, $\sim 1620 \text{ cm}^{-1}$ assigned to anionic C-O asymmetrical stretching, $\sim 1515 \text{ cm}^{-1}$ can be due to aromatic skeletal stretching vibration or phenol group benzene stretching, ~ 1422 and $\sim 1375 \text{ cm}^{-1}$ contributed to C-H bending, sharp absorption peak $\sim 1317 \text{ cm}^{-1}$ could be attributed to C-O symmetrical stretching, ~ 1150 , ~ 1075 , $\sim 1034 \text{ cm}^{-1}$ might be due to C-O stretching vibration [14,21]. The fingerprint region which showed a peak at ~ 781 , ~ 662 , $\sim 516 \text{ cm}^{-1}$ can be due to high levels of oxalate [21]. The 12 representative Guan-Mutong samples fulfill the key character absorption peaks of Guan-Mutong which are around $\sim 1318 \text{ cm}^{-1}$ and $\sim 781 \text{ cm}^{-1}$. Hence, the identity of Guan-Mutong samples has been confirmed.

There were some main characteristics markers that can be used to differentiate these two types of Chuan-Mutong and Guan-Mutong. For example, Guan-Mutong samples showed additional sharp peaks at ~ 1620 , 1317 , ~ 780 , $\sim 518 \text{ cm}^{-1}$. These significant peaks represent the presence of oxalate which less obvious in Chuan-Mutong while Chuan-Mutong samples showed peaks at ~ 1740 , ~ 1650 , 1510 , ~ 1458 , $\sim 1256 \text{ cm}^{-1}$ which are not found in Guan-Mutong samples (Figs. 2 and 3).

The vast difference between peak positions, intensities and the shapes of the peaks in the absorption bands between Chuan-Mutong and Guan-Mutong observed can be used to discriminate these two species. For example, Guan-Mutong showed a very sharp peak at $\sim 1620 \text{ cm}^{-1}$ which indicates a high level of oxalate [20,22]. Besides, Chuan-Mutong showed two significant low-intensity peaks at ~ 1740 and $\sim 1650 \text{ cm}^{-1}$ indicating the presence of ester which is not/less found in Guan-Mutong samples. Moreover, Chuan-Mutong samples showed a small and distinct peak at $\sim 1510 \text{ cm}^{-1}$ compared to Guan-Mutong samples which only showed a mild peak at $\sim 1520 \text{ cm}^{-1}$. This might indicate the level of ester is higher in Chuan-Mutong than Guan-Mutong. Furthermore, the analysis of FT-IR spectra revealed that only Chuan-Mutong samples showed absorption peaks at ~ 1650 and $\sim 1460 \text{ cm}^{-1}$ which infer the presence of more aromatic rings. Chuan-Mutong samples showed a relatively prominent ladder shape in the range of $1200\text{--}1000 \text{ cm}^{-1}$, indicating that it contained more starch as compared to the Guan-Mutong samples [15,22]. Moreover, there were some slight differences in the fingerprint region in the spectra of Chuan-Mutong and Guan-

Table 3

Peak assignment on the conventional FT-IR spectra of the Chuan-Mutong and Guan-Mutong.

Peak (cm^{-1})		Primary Assignment	Possible Compounds
Chuan-Mutong	Guan-Mutong		
~3376	~3341	O-H, ν	—
~2927	~2926	C-H, ν_{as}	—
~1736	~1735	C=O	Ester
~1647	~1620	Ring	Aromatic
		Anionic C-O, ν_s	Oxalate
~1510	~1515	Phenol group benzene, ν	Tannin (ester, glycoside, benzene)
		Ring	Aromatic
~1424	~1422	Ring	Aromatic
~1374	~1376	Ring	Aromatic
~1323		Phenol group O-H bending	Tannin (ester, glycoside, benzene)
	~1317	C-O, ν_s	oxalate
~1252	~1249	C-O, ν_s	lipid
~1157	~1154	C-O, ν	starch
~1110		C-O, ν	sucrose
~1050	~1100	C-O, ν	Tannin (ester, glycoside, benzene)
	~1034	C-O, ν	Tannin (ester, glycoside, benzene)
~896	~895	fingerprint	sucrose
	~781	C-O, ν	oxalate
~667	663	fingerprint	oxalate
~601		fingerprint	phosphate
~527	518	fingerprint	oxalate

Mutong. Two significant sharp and strong peaks at ~ 780 and $\sim 518 \text{ cm}^{-1}$ were only found in Guan-Mutong samples but not in Chuan-Mutong. Chuan-Mutong does not show significant peaks in the fingerprint region, whereas only mild peak range at ~ 605 and $\sim 530 \text{ cm}^{-1}$ are observed in Chuan-Mutong but absent in Guan-Mutong (Table 3).

SD-IR spectra were used to resolve overlapped bands in the original spectra and magnify minor differences between the samples. Figs. 4 and 5 showed the SD-IR spectra of Chuan-Mutong and Guan-Mutong, respectively in the range of $1800\text{--}400 \text{ cm}^{-1}$. This range was selected because it contained the main absorption bands of the chemical constituents of the Chuan-Mutong and Guan-Mutong. Five strong peaks at ~ 1621 , ~ 1317 , ~ 1160 , ~ 1079 , $\sim 782 \text{ cm}^{-1}$ were found in Guan-Mutong samples (Fig. 5), whereas only four strong peaks at ~ 1514 , ~ 1469 , ~ 1164 , and $\sim 897 \text{ cm}^{-1}$ were found in Chuan-Mutong samples (Fig. 4). Hence, the identity of Guan-Mutong and Chuan-Mutong samples has been confirmed through SD-IR.

3.3. 2D-IR spectrum of Chuan-Mutong and Guan-Mutong

2D-IR can be used to abstract possible information of the intra-molecular and inter-molecular interactions of the functional groups for the purpose of discriminating Chuan-Mutong against Guan-Mutong. It has the possible advantage of deriving additional information on the temperature sensitivity of the specific chemical components in the herbal samples. Moreover, 2D-IR provides a more precise information on the resolution and response of the chemical functional groups regarding different thermal perturbations [15] as compared to the conventional FT-IR spectra method. Hence, 2D-IR provides an alternative, independent and complementary validation in the discrimination of Chuan-Mutong and Guan-Mutong to the conventional FT-IR for analyzing the chemical components in the herbal samples.

Fig. 6 showed the synchronous 2D-IR spectra of Chuan-Mutong in the range of $1750\text{--}1500 \text{ cm}^{-1}$. Most of the Chuan-Mutong samples showed 4 major autopeaks at ~ 1517 , ~ 1595 , ~ 1650 and $\sim 1717 \text{ cm}^{-1}$, and the autopeaks observed are very sharp. These major autopeaks reflect the positive cross-peaks correlated to each other with the increasing

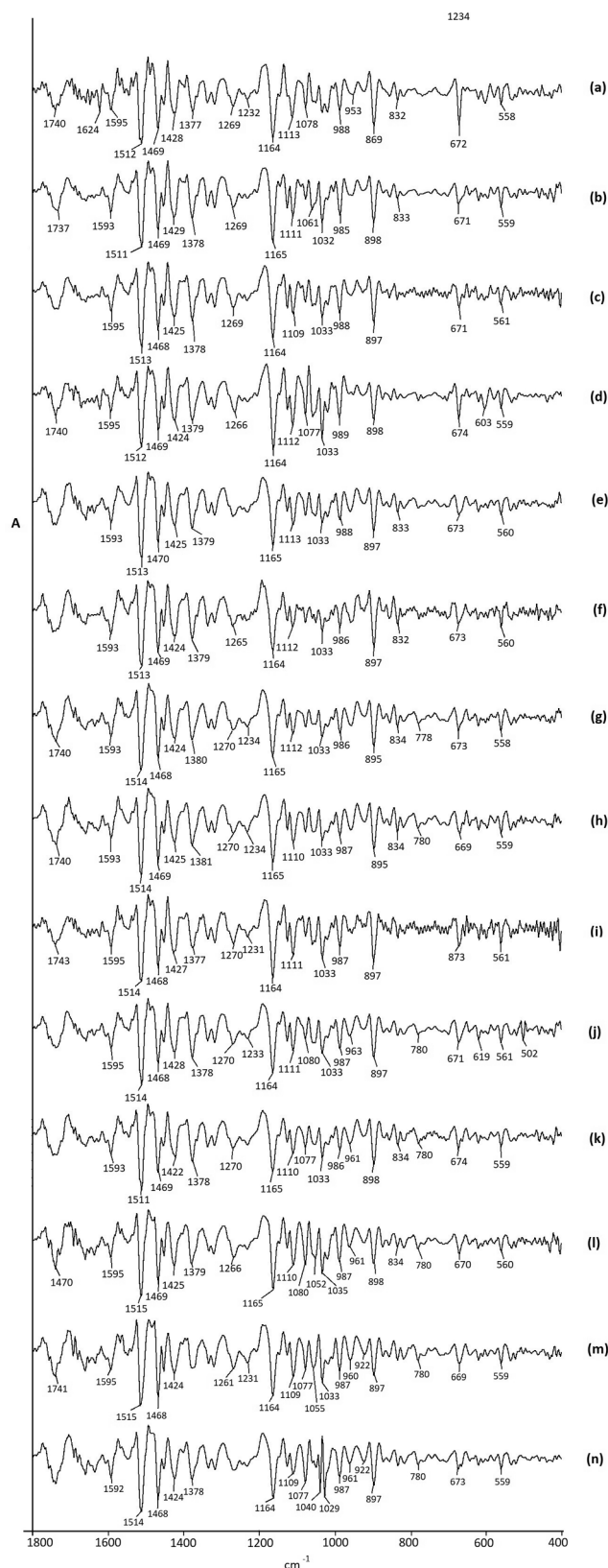


Fig. 4. Second derivatives IR spectrum of Chuan-Mutong from Malaysia and China: (a) T01, (b) S08, (c) SB02, (d) PP05, (e) PK13, (f) PH08, (g) NS10, (h) KL10, (i) KT04, (j) K09, (k) J10, (l) C13, (m) STD 01, (n) NFDC (National Institute for Food and Drug Control (Beijing, China)).

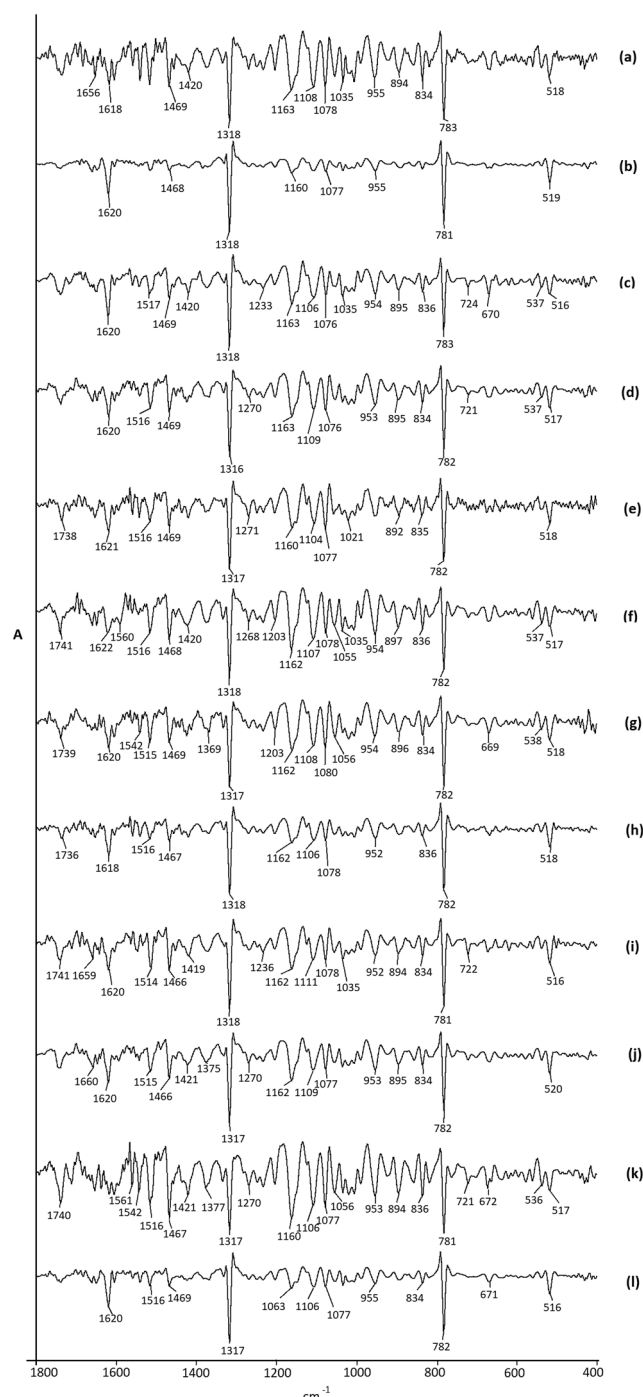


Fig. 5. Second derivatives IR of Guan-Mutong from Malaysia and China: (a) S07, (b) PP07, (c) P01, (d) PK14, (e) NS13, (f) M01, (g) KT03, (h) PH07, (i) KL06, (j) K12, (k) J11, (l) C16.

temperature and indicate the chemical compounds have similar thermal stability. The 4 sharp autopeaks might be the characteristics markers to indicate the presence of a large amount of inorganic minerals which include aromatic substances.

On the other hand, Guan-Mutong samples showed lesser major autopeaks as compared to Chuan-Mutong. There are only 2 major and important autopeaks found in most of the Guan-Mutong samples which are at $\sim 1580\text{ cm}^{-1}$ and $\sim 1650\text{ cm}^{-1}$ (Fig. 7). The absence of overlapped peaks could be a distinct marker to distinguish between Chuan-Mutong and Guan-Mutong. The difference in the autopeak positions, intensities, and the relative cross peak of diagonals between Chuan-Mutong and

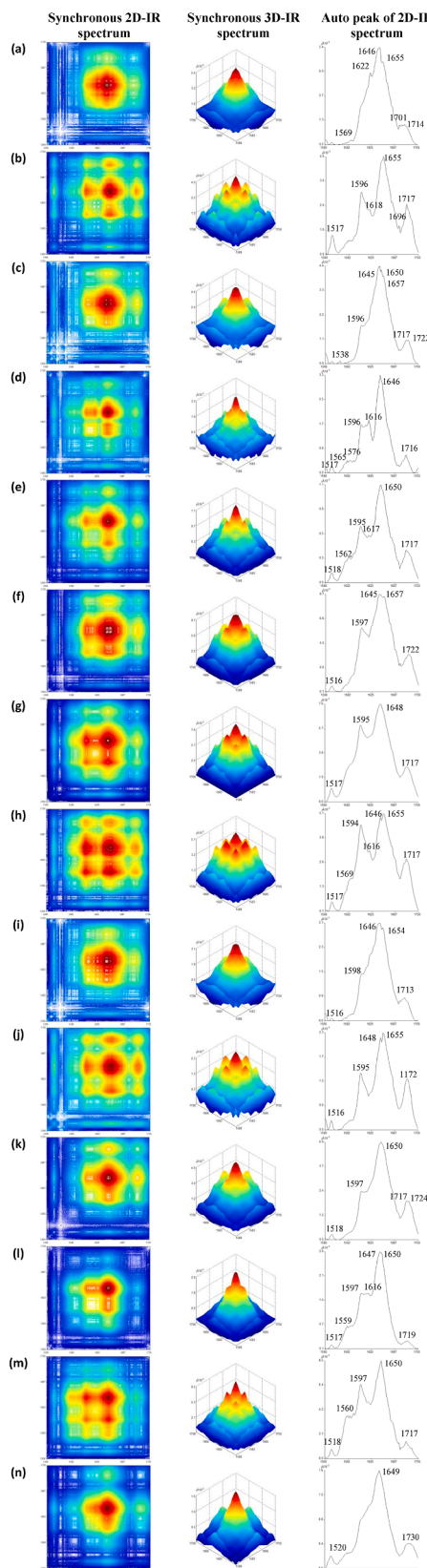


Fig. 6. Synchronous 3D and 2D-IR spectrum, and auto peak of 2D-IR of Chuan-Mutong from Malaysia and China:(a) T01, (b) S08, (c) SB02, (d) PP05, (e) PK13, (f) PH08, (g) NS10, (h) KL10, (i) KT04, (j) K09, (k) J10, (l) C13, (m) STD 01, (n) NFDC (National Institute for Food and Drug Control (Beijing, China)).

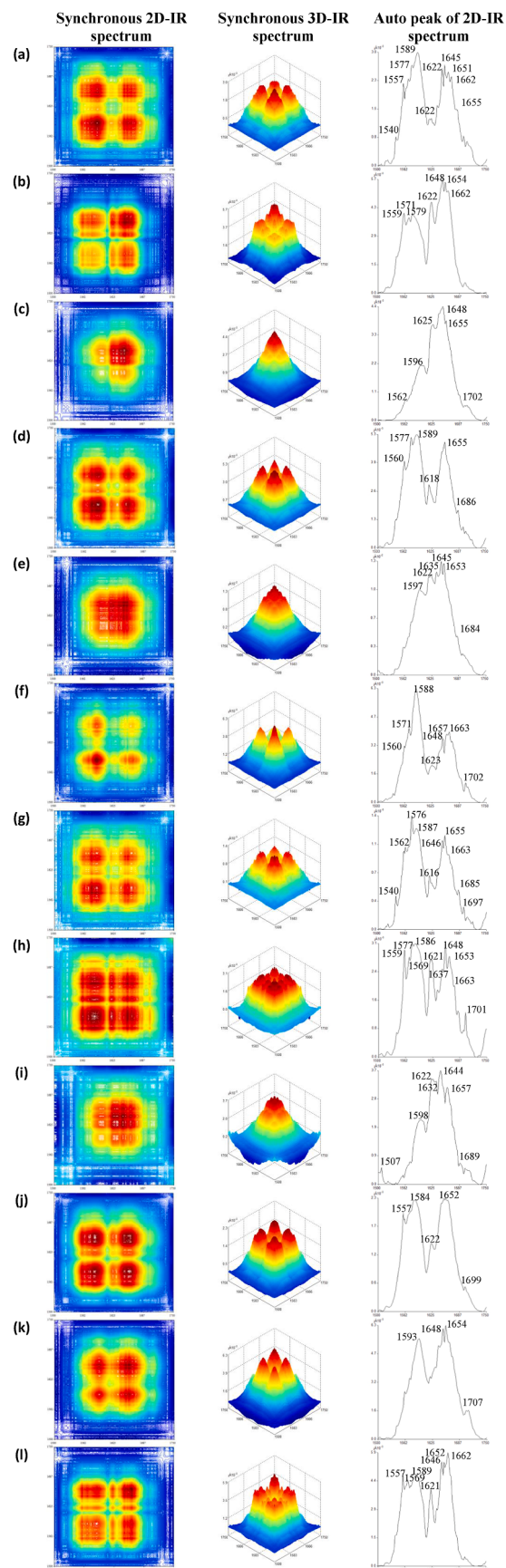


Fig. 7. Synchronous 3D and 2D-IR spectrum, and auto peak of 2D-IR of Guan-Mutong from Malaysia and China: (a) S07, (b) PP07, (c) P01, (d) PK14, (e) NS13, (f) M01, (g) KT03, (h) PH07, (i) KL06, (j) K12, (k) J11, (l) C16.

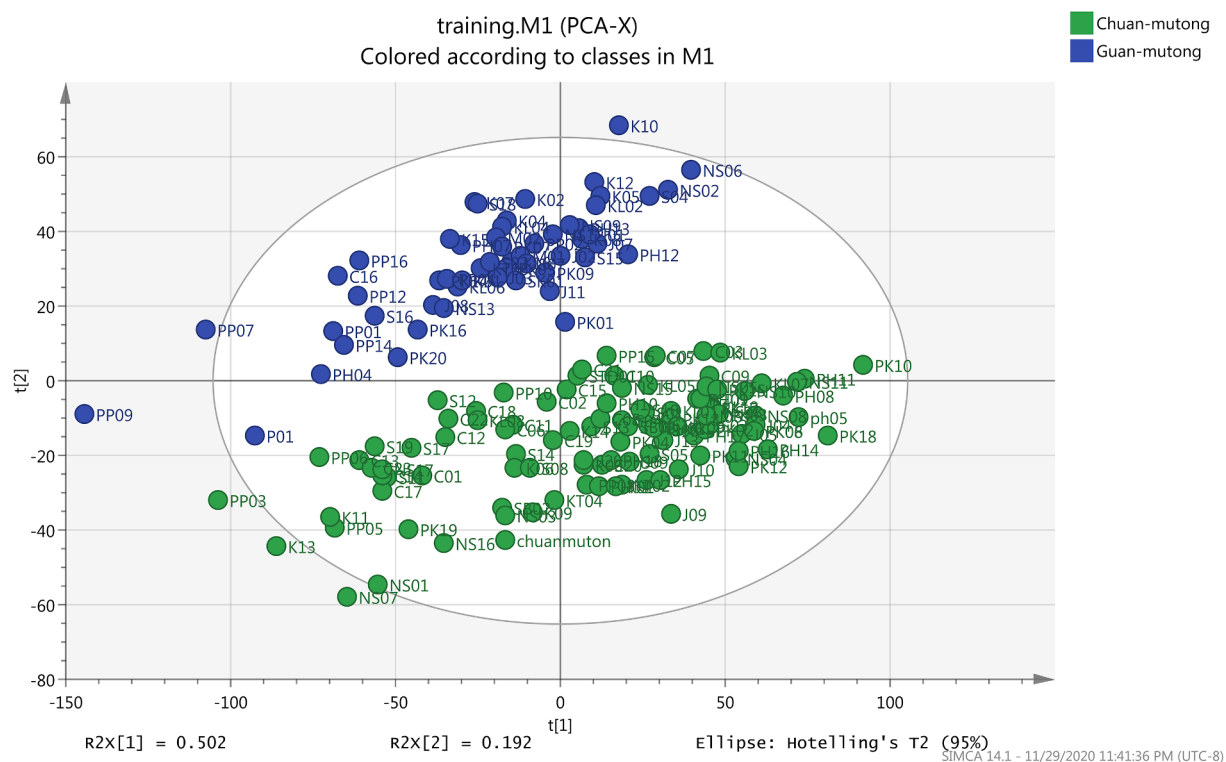


Fig. 8. PCA score scatter plot of mutong.

Table 4
The parameters of PLS-DA model.

	R^2Y	Q^2Y	RMSEE	RMSEC	RMSECV	Sensitivity	Accuracy	Specificity
Mutong	0.992	0.982	0.0963397	0.11679	0.15369	100%	100%	100%

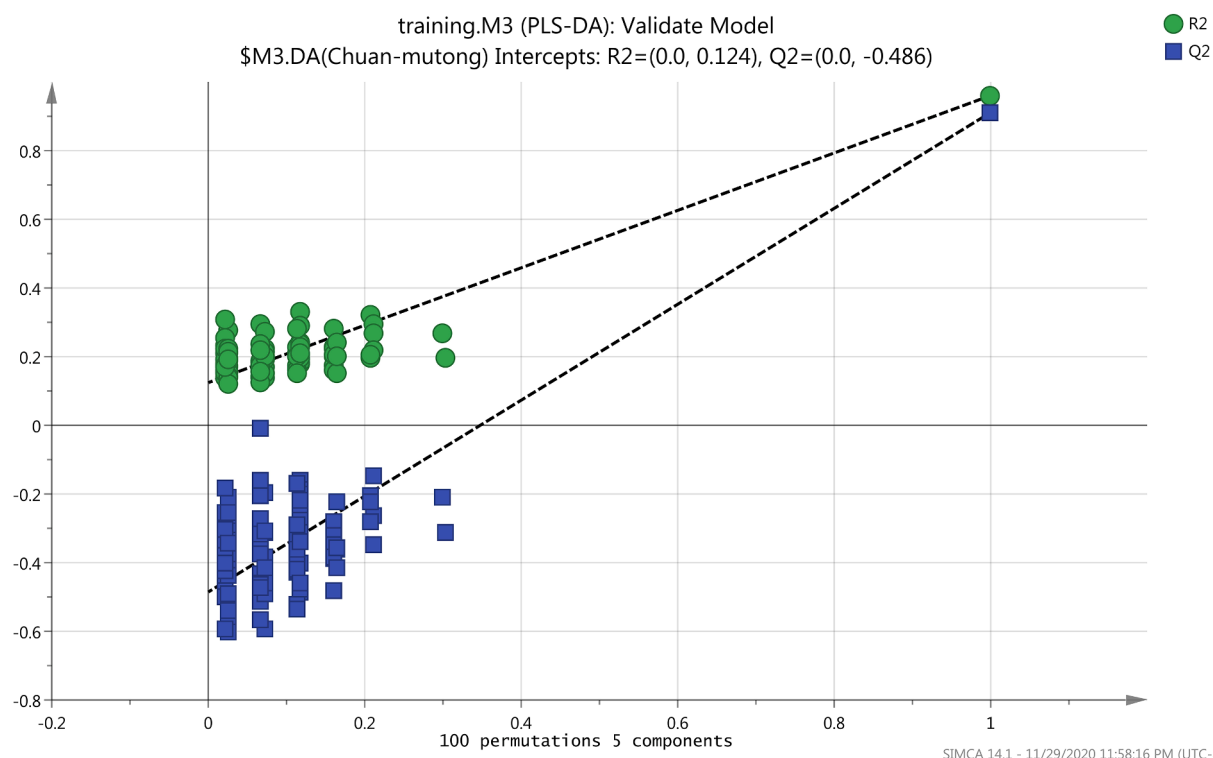


Fig. 9. The permutation test of PLS-DA model.

Material	Sensitivity (in %)										Specificity (in %)													
	Machine learning classifier					Random Forests					J48					RBF Classifier			Random Forests			J48		
	Lower Bound	Mean	Upper Bound	Lower Bound	Mean	Upper Bound	Lower Bound	Mean	Upper Bound	Lower Bound	Mean	Upper Bound	Lower Bound	Mean	Upper Bound	Lower Bound	Mean	Upper Bound	Lower Bound	Mean	Upper Bound	Lower Bound	Mean	Upper Bound
Guan-Mutong	91.57	91.99	92.36	92.06	92.48	92.84	98.61	99.03	99.39	92.96	93.36	93.76	92.96	93.36	93.73	99.17	99.48	99.75	98.61	99.03	99.39	98.61	99.03	99.39
Chuan-Mutong	92.96	93.36	93.76	92.96	93.36	93.73	99.17	99.48	99.72	91.57	92.00	92.36	92.06	92.48	92.84	98.61	99.03	99.39	98.61	99.03	99.39	98.61	99.03	99.39

Guan-Mutong can be easily discriminated by 2D-IR ([Figs. 6 and 7](#)).

3.4. Chemometrics analysis and differentiation of Chuan-Mutong and Guan-Mutong

Principle Component Analysis (PCA) is one of the biometrics methods to extract the characteristic features and transform original correlated variables into a series of uncorrelated variables to create a data set. The combination of variables is then used as a reference to identify the samples. This method is used to reduce the complexity of data by applying a set of PCA algorithms which includes standard deviation, covariance, and eigenvectors. In this study, the FT-IR spectrum of each sample is normalized to carry out the PCA analysis. The result of 164 herb samples subjected to PCA analysis are shown in [Fig. 8](#), which indicates that the samples are significantly separated into two distinct groups. The first two PCs accounted for 69.42% (PC1 = 50.17% and PC2 = 19.25%) for the samples. Most of the Chuan-Mutong samples are clearly separated from the Guan-Mutong. The Chuan-Mutong spectra belonged to one cluster and the Guan-Mutong spectra belonged to another separate cluster. Thus, the PCA results indicated the good performance and rationality of the FT-IR fingerprint [[17](#)].

The FT-IR data was processed with the PLS-DA (SIMCA 14.1, Umetric, Sweden). PLS-DA is a linear pattern classification method widely used to deal with complicated data matrices by dimension reduction. Results shown in [Table 4](#), the R^2Y and Q^2Y of the spectra were 0.992 and 0.982, respectively. With the R^2Y and Q^2Y cross-validation values >0.9 and the difference between these value <0.1 indicated that the model has excellent fit and very high predictive performance. In response permutation test, R^2Y and Q^2Y were 0.124 and -0.486 , respectively ([Fig. 9](#)). The R^2Y and Q^2Y the values were <0.3 and <0.05 , respectively, indicated that the model is a perfect fit to one another and the data are a good model. RMSE for training data RMSEP for test data were similar (0.09633 and 0.11679, respectively) and low RMSECV (0.15367) again indicated that the built model is good. The sensitivity, accuracy and specificity of the model are 100%.

3.5. Machine learning classifier analysis

Three adopted classifiers are able to yield high accuracy rates ($>95\%$) under the 10-fold cross-validation method. The mean accuracy rates of classifiers are above 92%. In addition, the Area Under the receiver operating characteristics (AUC) is computed, where an AUC score of 1 represents a perfect performance. Based on the results, all three classifiers produce high AUC scores (>0.8). It is worth noting that the AUC metric measures discrimination, which is the ability to classify correctly both Guan-Mutong and Chuan-Mutong.

We further ascertain the results (both accuracy rates and AUC scores) using the bootstrap analysis, which is useful to approximate the statistical distribution of the 30-runs results under random sampling. The bootstrapped results and their 95% confidence interval (indicated as the lower and upper bounds) are computed with 1,000,000 resamplings.

It can be observed that the same group of classifiers achieves high AUC scores (>0.9). The analysis implies that these classifiers have the capability of classifying both Guan-Mutong and Chuan-Mutong as shown in [Table 5](#). Even though the sensitivity results from machine learning classifiers were slightly lower compared to PLS-DA, the scores are still higher than 91%. This indicates that the machine learning classifiers achieve a high level of recognition ability for each tested material. The specificity results of machine learning classifiers show high values range of 91.57 to 99.48% compared to PLS-DA (100%) ([Table 5](#)).

Machine learning models are useful for the classification of the Chuan-Mutong and Guan-Mutong, as ascertained by the high accuracy rates. The results indicate that the classified Chuan-Mutong and Guan-Mutong are closely similar to those obtained from the physical experiments. The performance is supported with high AUC scores, which

Table 6

Bootstrapped accuracy rate and AUC score of machine learning classifier.

Classifier	Bootstrapped Accuracy Rate (in %)			Bootstrapped AUC Score (average for classes)		
	Lower Bound	Mean	Upper Bound	Lower Bound	Mean	Upper Bound
RBF Classifier	92.56	92.21	92.78	0.9797	0.9851	0.9896
Random Forests	92.78	93.07	93.23	0.8363	0.8475	0.8504
J48	99.08	99.32	99.53	0.8413	0.8475	0.8535

vindicate that the classifiers have the capability of discriminating against the known Chuan-Mutong and Guan-Mutong, in agreement with the physical experiments (Table 6). The present study has demonstrated the potential of machine learning classifiers as a useful tool for differentiating Chuan-Mutong from Guan-Mutong. The finding serves as a foundation to conduct further investigations into the use of machine learning for pharmaceutical product development.

4. Conclusion

This research study shows the reliability of the infrared spectroscopic tri-step identification approach to rapidly identify the Chuan-Mutong, Guan-Mutong and Mutong relate species. Based on the peak shapes, peak positions, and peak intensities on FT-IR and SD-IR spectra, these three types of herbs can be unambiguously differentiated. 2D-correlated IR is further used to validate the authenticity of the differentiation of the sample herbs. This method is safe, qualitative, and non-destructive for discriminating the sample herbs to ensure the quality, safety, and efficacy of Chuan-Mutong and Guan-Mutong in clinical usage. Overall, PCA, PLS-DA and ML classifiers can effectively discriminate Chuan-Mutong and Guan-Mutong species against unidentified species.

Declaration of Competing Interest

The authors declare that they have no known competing financial interests or personal relationships that could have appeared to influence the work reported in this paper.

Acknowledgements

The research was supported by Yam Mun Fei Research Fund, Fujian Provincial Finance Project-Fujian Academy of Agricultural Sciences Innovation Team Construction Project (STIT2017-2-8), Fujian Academy of Agricultural Sciences Productive Engineering Laboratory Construction Project (2015GCH-6). Dr Tiem Leong Yoon acknowledges the courtesy of Wawasan Open University for hosting his sabbatical leave

during which part of this work was carried out. The authors would like to acknowledge the students (Bachelor of Pharmacy (batch 2015-2019)) who helped in sample collection.

References

- [1] Committee, P., Pharmacopoeia of the People's Republic of China, China Medical Science Press, Beijing, China, 2010.
- [2] L. Wu, B. Wang, M. Zhao, W. Liu, P. Zhang, Y. Shi, C. Xiong, P. Wang, W. Sun, S. Chen, Rapid Identification of officinal *Akebiae Caulis* and its toxic adulterant *Aristolochiae Manshuriensis Caulis* (*Aristolochia manshuriensis*) by loop-mediated isothermal amplification, R. Front Plant Sci. 20 (7) (2016) 887.
- [3] H.J. Jung, et al., Structure-activity relationship of oleanane disaccharides isolated from *Akebia quinata* versus cytotoxicity against cancer cells and NO inhibition, Biol. Pharm. Bull. 27 (2004) 744–747.
- [4] G.M. Lord, et al., Nephropathy caused by Chinese herbs in the UK, Lancet 354 (1999) 481–482.
- [5] Y. Zhu, Toxicity of the Chinese herb Mu Tong (*Aristolochia manshuriensis*) what history tells us, Adverse Drug React. Toxicol. Rev. 21 (2002) 171–177.
- [6] L.J. Vanherweghem, Misuse of herbal remedies: the case of an outbreak of terminal renal failure in Belgium (Chinese herbs nephropathy), J. Altern. Complement. Med. 4 (1998) 9–13.
- [7] T.G. Chui, H.Y. Wang, Study on the effect of pharmacopoeia's legal dosage guan mutong on renal function and interstitial structure in rats, Chinese J. Nephrol. 16 (2000) 103–106.
- [8] B.Q. Zhou, D. Zhao, General situation and analysis on the side effects of Mutong, Inner Mongolia Traditional Chinese Medicine 23 (2004) 37–39.
- [9] X.N. Chen, Discussion on the medicinal standards for the abolishment of Chinese medicine containing aristolochic acid, China Pharmacy 18 (2007) 2321–2322.
- [10] H.M. Ma, B.L. Zhang, Research and clinical application of Mutong's herbal medicine, Zhejiang J. Traditional Chinese Med. 36 (2001) 533–534.
- [11] H.M. Ma, B.L. Zhang, The research on the history of mutong types, Tian Jin Chinese Medicine College, Tian Jin, China, 2001.
- [12] J.K. Chen, T.T. Chen, Chinese medical herbology and pharmacology, Art of Medicine Press, CA, USA, 2001.
- [13] J.M.A. van der Valk, J.L. Christine, N. Mark, Macroscopic authentication of Chinese materia medica (CMM): A UK market study of seeds and fruits, J. Herbal Med. 8 (2017) 40–51.
- [14] Y.S. Ch'ng, et al., Vasorelaxation study and tri-step infrared spectroscopy analysis of Malaysian local herbs, J. Pharmacopuncture 19 (2016) 145–154.
- [15] Y. Chen, et al., Rapid authentication and identification of different types of *A. roxburghii* by Tri-step FT-IR spectroscopy, Spectrochim. Acta, Part A 199 (2018) 271–282.
- [16] K.H. Wong, et al., Differentiation of *Pueraria lobata* and *Pueraria thomsonii* using partial least square discriminant analysis (PLS-DA), J. Pharm. Biomed. Anal. 84 (2013) 5–13.
- [17] H. Abdi, L.J. Williams, Principal component analysis. Wiley interdisciplinary reviews: computational statistics, 2 (2010) 433–459.
- [18] L. Breiman, Random Forests, Machine Learning 45 (2001) 5–32.
- [19] F. Schwenker, H.A. Kestler, G. Palm, Three learning phases for radial-basis-function networks, Neural Networks 14 (2001) 439–458.
- [20] S.S. Gao, et al., Development of FTIR fingerprint for identification of armand clematis stem (chuanmutong) and realted herbs, China J. Chinese Materia Medica 41 (2016) 1485–1492.
- [21] S.Q. Sun, Q. Zhou, J.B. Chen, Infrared Spectroscopy for Complex Mixtures: Applications in Food and Traditional Chinese Medicine, Chemical Industry Press, Beijing, China, 2011.
- [22] C.H. Ng, et al., Application of mid-infrared spectroscopy with multivariate analysis for the discrimination of toxic plant, *Gelsemium elegans*, Vibrational Spectroscopy 99 (2018) 13–24.